OPEN ACCESS
Saudi Journal of Civil Engineering
Abbreviated Key Title: Saudi J Civ Eng
ISSN 2523-2657 (Print) |ISSN 2523-2231 (Online)
Scholars Middle East Publishers, Dubai, United Arab Emirates
Journal homepage: https://saudijournals.com/journal/sjce/home

Original Research Article

Reliability-Based Optimisation of Cement-Replacing Steel Fibre Dosage in Concrete: A Mechanistic Model Linking Compressive Strength, Characteristic Strength and Structural Reliability

Rowland-Lato Eghosasere Oluwaseyi[1]*

[1]Department of Civil Engineering, University of Port Harcourt, Rivers State, Nigeria

DOI: https://doi.org/10.36348/sjce.2026.v10i07.001 | **Received:** 28.05.2026 | **Accepted:** 16.07.2026 | **Published:** 21.07.2026

***Corresponding author:** Rowland-Lato Eghosasere Oluwaseyi
Department of Civil Engineering, University of Port Harcourt, Rivers State, Nigeria

Abstract

Steel fibre-reinforced concrete (SFRC) is generally modelled for compressive strength; nevertheless, almost all published models assume fibres are added to a fixed mix and stop at predicting mean strength, neglecting both the cement-replacement scenario and reliability-based design. This study develops a mechanistic, interpretable model for SFRC in which steel fibres replace cement by mass, a composition that raises the effective water-to-cement ratio while incorporating crack-bridging benefit. Compressive strength is expressed as the sum of a paste-weakening term decaying with the surviving cement fraction and a Rayleigh-type bridging term that peaks before balling degrades dispersion. Across seven fibre dosages (0–12% of cement mass) at two curing ages (224 specimens), the model reproduced the non-monotonic strength response with $R^2 = 0.887$ at 28 days and independently recovered the bridging optimum near 6–7% fibre without that value being imposed, indicating that it demonstrates the governing physics rather than merely fitting the data. Hardened density showed no reliable dosage trend and stayed within the normal-weight band. Extending the study to characteristic strength and reliability indices, the model showed that only the control mix cleared the design target, every fibre mix falling below it. The framework links predictive accuracy to structural usability, with external validation identified as the priority next step.
Keywords: steel fibre-reinforced concrete; cement replacement; compressive strength prediction; mechanistic modelling; structural reliability; characteristic strength.

1. INTRODUCTION

Steel fibre-reinforced concrete (SFRC) has become a mainstream structural material, and the accurate prediction of its hardened properties chiefly compressive strength and density remains an active research problem. Over the period 2020–2026, the modelling of these properties has been transformed by the widespread adoption of machine learning (ML), which has largely displaced the earlier reliance on empirical regression. The most conspicuous trend is the decisive move away from purely empirical formulae toward data-driven models; Ben Chaabene *et al.,* (2020) argued in an influential critical review that conventional empirical models are frequently inaccurate and inflexible, positioning ML as the natural successor while cautioning against careless model selection.

Despite this progress, three gaps persist. First, density prediction for SFRC is comparatively neglected, being almost always treated as a model input or controlled design target rather than a predicted output. Second, almost all published models assume that fibres are *added* to a fixed mix; the practically important scenario in which fibres partially *replace* cementitious content, thereby raising the effective water-to-cement ratio, is essentially unmodelled. Third, most models stop at predicting mean strength and do not propagate their predictions to the characteristic strength and reliability indices that structural design actually requires.

This study addresses all three. It develops a transparent, mechanistically derived model in which steel fibres replace cement by mass, calibrates it against a controlled programme of seven fibre dosages at two curing ages, honestly assesses density, and propagates the calibrated strength model to characteristic strength and structural reliability. The approach is deliberately first-principles: every equation is built from a physical mechanism, each term is justified before it is written, and the resulting model is tested against the measured data, with terms discarded where the data do not support them.

2. LITERATURE REVIEW

2.1 The shift toward machine learning and reported accuracy

Subsequent SFRC-specific studies bore out the shift toward data-driven models. Kang *et al.,* (2021) applied roughly a dozen algorithms to predict compressive and flexural strength and found that tree-based and boosting methods, particularly extreme gradient boosting, clearly outperformed linear regression, K-nearest neighbours and multilayer perceptrons. Reported accuracies for compressive-strength prediction are consistently high, typically ranging from $R^2 \approx 0.85$ to 0.96. Li *et al.,* (2022) combined support vector regression with AdaBoost and bagging and reported the AdaBoost variant as best ($R^2 \approx 0.96$). Pakzad *et al.,* (2023) compared several algorithms on 176 hooked-steel-fibre records, finding that a convolutional neural network was the most accurate ($R^2 = 0.928$). Al-Shamasneh *et al.,* (2025) benchmarked six regressors on a larger dataset of 600 points and identified Gaussian process regression as the best model ($R^2 = 0.93$). Across these studies, ensemble and kernel-based learners consistently outperform simple linear and instance-based methods.

2.2 Interpretable and evolutionary models

Alongside black-box learners, evolutionary methods that yield an explicit predictive equation have gained traction. Alyousef *et al.,* (2023) compared adaptive neuro-fuzzy inference systems, artificial neural networks and gene expression programming for the compressive strength of SFRC at elevated temperatures, reporting gene expression programming as clearly superior, and found through a Shapley additive explanation analysis that cement content, temperature and water-to-cement ratio together accounted for the large majority of feature importance. Artificial neural networks remain widely used: Mahesh and Sathyan (2022) modelled multiple hardened SFRC properties, while Premkumar and Senthil Selvan (2025) trained a network on 967 datapoints to predict several mechanical properties simultaneously. Response surface methodology continues to serve optimisation studies (Köksal *et al.,* 2022), and reference-database construction has been advanced by Wang *et al.,* (2022) and by the meta-analysis of Garcia-Taengua *et al.,* (2021).

2.3 Controversies and gaps

A consistent finding is that the water-to-cement ratio, cement and superplasticiser content, supplementary cementitious materials and curing age dominate compressive-strength predictions, whereas steel-fibre descriptors tend to rank lower (Pakzad *et al.,* 2023; Alyousef *et al.,* 2023). This feeds the central controversy over whether steel fibres materially change compressive strength at all (Kang *et al.,* 2021). Further debates concern the tension between predictive accuracy and interpretability (Abbas & Khan, 2023), and the reliability of high accuracies reported on small, non-standardised datasets (Ben Chaabene et al., 2020; Wang *et al.,* 2022). Dedicated density-prediction models are rare, the most relevant addressing lightweight or foamed concrete rather than steel-fibre concrete (Ullah *et al.,* 2022; Stel'makh *et al.,* 2022). The modelling of fibres as a cement replacement, coupled strength–density formulations, and mechanistic treatments of the associated water-to-cement penalty remain the most significant opportunities for original contribution.

3. MATERIALS AND METHODS

3.1 Experimental programme

The programme tested 150 mm cube specimens at seven fibre replacement levels (0, 2, 4, 6, 8, 10 and 12% of cement mass), with all other mixture constituents and testing protocols held constant. This parametric approach isolates the effect of fibre content on compressive strength, statistical variability and reliability. For each fibre content, specimens were tested at two curing ages (7 and 28 days), with primary analysis focusing on 28-day results consistent with structural design practice. Sixteen replicate specimens per condition were prepared, yielding a total of 224 cube specimens in the experimental programme (7 fibre contents × 2 ages × 16 replicates).

3.2 Materials

Ordinary Portland Cement conforming to ASTM C150 and equivalent to CEM I 42.5R under BS EN 197-1 was used throughout, sourced from a single batch to eliminate inter-batch variability. Fine aggregate was Zone II river sand (fineness modulus 2.65) conforming to ASTM C33, and coarse aggregate conformed to the same specification. The mix was designed as an M30 concrete with a design water-to-cement ratio of 0.500. Discrete steel fibres were used at replacement levels defined by mass of cement.

3.3 Mix design and the cement-replacement mechanism

Fibres replaced cement by mass while the water content was held constant. The original cement mass per cube was 5.114 kg and the water mass 2.557 kg. Replacing a fibre fraction p of the cement reduces the cement to $5.114(1-p)$ while leaving water unchanged, so the effective water-to-cement ratio rises. Table 1 presents the mix design for all seven replacement levels.

Table 1: M30 concrete mix design with steel fibre replacement (per 150 mm cube)

Fibre %	Original cement (kg)	Fibre (kg)	New cement (kg)	Water (kg)	Sand (kg)	Coarse (kg)	New w/c
0	5.114	0.000	5.114	2.557	7.670	10.227	0.500
2	5.114	0.102	5.011	2.557	7.670	10.227	0.510
4	5.114	0.205	4.909	2.557	7.670	10.227	0.521
6	5.114	0.307	4.807	2.557	7.670	10.227	0.532
8	5.114	0.409	4.705	2.557	7.670	10.227	0.543
10	5.114	0.511	4.602	2.557	7.670	10.227	0.556
12	5.114	0.614	4.500	2.557	7.670	10.227	0.568

4. MODEL DEVELOPMENT

4.1 The controlling physical idea

The single most important fact about this mix design is that fibres replace *cement*, but the water content is fixed. Removing cement while keeping water constant raises the effective water-to-cement ratio. If p is the fibre fraction of the original cement mass, the new cement mass is $m_{c,0}(1-p)$ and the water-to-cement ratio becomes

$$\frac{w}{c}(p) = \frac{w_0}{c_0\,(1-p)} = \frac{0.500}{1-p} \qquad (1)$$

Equation (1) reproduces the adjusted ratios in Table 1 exactly (0.500 at $p = 0$ rising to 0.568 at $p = 0.12$). This is the mechanism behind the systematic loss of strength: less binder holding the same amount of water produces a weaker, more porous paste. Working against it, discrete steel fibres bridge micro-cracks and transfer stress across them, recovering some capacity. This benefit grows with fibre content at low dosages but saturates and then reverses at high dosages, where balling and poor dispersion introduce defects. The strength of SFRC is therefore the result of two competing mechanisms that share a single master variable, p.

4.2 Why a single classical law is insufficient

The classical Abrams relationship expresses strength as a function of water-to-cement ratio alone,

$$f_{cu} = \frac{A}{B^{w/c}} \qquad (2)$$

Fitting Equation (2) to the 28-day data yields only $R^2 \approx 0.27$. It captures the average downward drift but cannot reproduce the observed dip at 2%, the recovery to a peak near 6%, and the subsequent gentle decline. A monotonic law in w/c cannot describe a non-monotonic response, so a second mechanism must be introduced explicitly.

4.3 Building the two-mechanism model

The first mechanism, weakening of the paste as cement is removed, is written as a decay in $(1-p)$, the surviving cement fraction:

$$f_{\text{paste}}(p) = f_{c0}\,(1-p)^m \qquad (3)$$

Here f_{c0} is the strength of the control paste and the exponent m measures how sharply strength falls as binder is lost. The second mechanism, crack bridging, must rise from zero, reach a maximum, then decline as balling degrades the benefit. The simplest single-peaked function with this shape is the Rayleigh-type term

$$f_{\text{bridge}}(p) = B_f\, p\, e^{-p/p_c} \qquad (4)$$

which is zero at $p = 0$, rises, and peaks precisely at $p = p_c$ before decaying. The coefficient B_f scales the bridging contribution and p_c locates the optimum dosage. Adding the two mechanisms gives the complete predictive model for compressive strength:

$$f_{cu}(p) = f_{c0}\,(1-p)^m + B_f\, p\, e^{-p/p_c} \qquad (5)$$

4.4 Density model

Density should be governed by a rule of mixtures. Replacing cement (specific gravity ≈ 3.15) with steel fibres (specific gravity ≈ 7.85) adds mass to a fixed volume, which should raise density in proportion to the fibre volume fraction V_f. In opposition to this, the rising water-to-cement ratio increases capillary porosity, which lowers density. The candidate model is therefore

$$\rho(p) = \rho_0 + \alpha\, V_f - \beta\left(\frac{w}{c} - 0.50\right) \qquad (6)$$

where ρ_0 is the control density, α scales the mass gain from added steel, and β scales the porosity penalty. The fibre volume fraction follows from the fibre mass and the steel and specimen volumes:

$$V_f = \frac{p\, m_{c0}/\rho_{\text{steel}}}{V_{\text{cube}}} \qquad (7)$$

4.5 Characteristic strength and reliability

For structural use, the mean is not enough; the lower-fractile (characteristic) strength governs. Assuming a normal distribution, the 5% characteristic value is

$$f_{ck} = \bar{f}_{cu} - 1.645\,\sigma \qquad (8)$$

and the reliability of each mix relative to the 30 N/mm² design target is measured by the index

$$\beta = \frac{\bar{f}_{cu} - f_{\text{target}}}{\sigma} \qquad (9)$$

5. RESULTS AND DISCUSSION

5.1 Density of hardened concrete

Table 2 presents the hardened-density results. Values ranged from 2289 to 2732 kg/m³ across all fibre percentages and curing ages, with the control at 2446 kg/m³ (28 days), within the accepted normal-weight range of 2300–2500 kg/m³.

Table 2: Hardened density results

Fibre %	w/c ratio	Density 7 d (kg/m³)	Density 28 d (kg/m³)	Change vs control (%)
0	0.500	2412	2446	0.0
2	0.510	2532	2732	+8.4
4	0.521	2413	2593	+3.0
6	0.532	2586	2541	+5.6
8	0.543	2579	2289	+0.2
10	0.556	2596	2492	+4.7
12	0.568	2467	2560	+3.5

When Equation (6) is fitted to the 28-day densities, the mechanistic trend is real but weak: the measured scatter overwhelms the systematic signal, and the coefficient of determination collapses to $R^2 \approx 0.09$. The scientifically defensible conclusion is that fibre replacement over this range does not produce a reliable, predictable density trend. Instead, the density remains bounded within the normal-weight concrete band,

$$\rho(p) \approx \bar{\rho} \pm \sigma_\rho, \qquad \bar{\rho} \approx 2520\ \mathrm{kg/m^3},\ \sigma_\rho \approx 130\ \mathrm{kg/m^3} \qquad 10)$$

Equation (10) is the appropriate predictive statement for density: a bounded mean rather than a false functional trend, more useful to a designer than an overfitted curve that scatter would render meaningless.

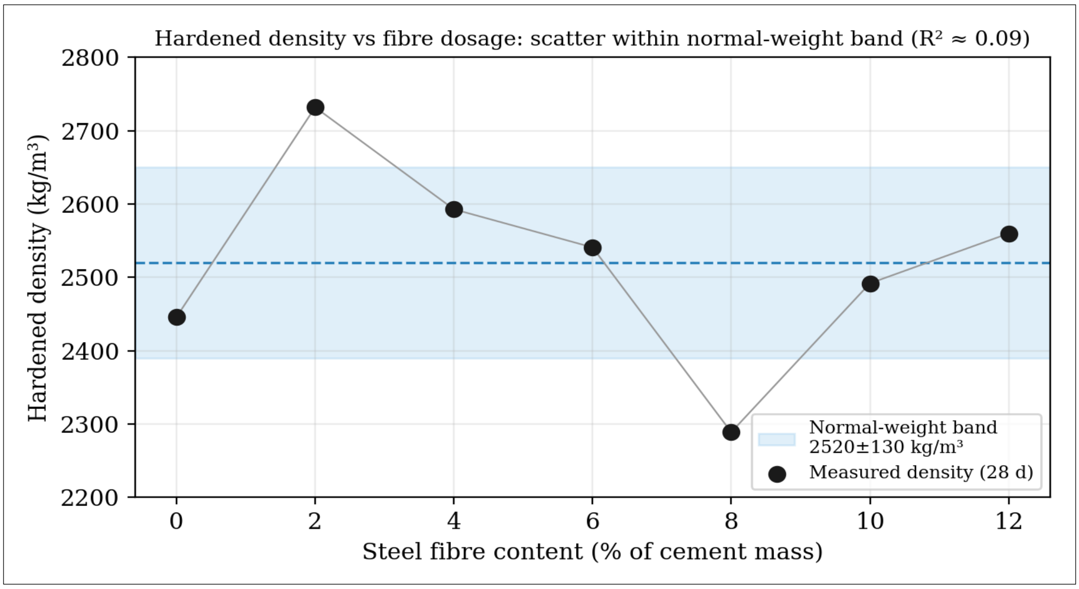

Figure 1: Hardened density versus fibre dosage at 28 days, shown against the normal-weight band; scatter dominates any systematic trend ($R^2 \approx 0.09$)

5.2 Compressive strength

Table 3 presents the mean compressive-strength results. The control achieved 33.45 N/mm² at 7 days and 42.15 N/mm² at 28 days. Fibre replacement produced substantial strength reductions across all dosages, with the 6% mix the strongest in the fibre series.

5.3 Calibration and performance of the strength model

Fitting Equation (5) to the measured mean cube strengths gives the coefficients in Table 4.

Table 3: Compressive strength results and characteristic values

Fibre %	w/c	7 d (N/mm²)	28 d (N/mm²)	f_ck 28 d (N/mm²)	Change vs control 28 d (%)
0	0.500	33.45	42.15	38.69	0.0
2	0.510	19.95	21.60	16.27	−48.7
4	0.521	24.95	26.50	21.69	−37.1
6	0.532	26.80	31.25	27.14	−25.9
8	0.543	24.25	25.65	19.60	−39.1
10	0.556	20.25	24.25	19.11	−42.5
12	0.568	23.55	25.60	20.91	−39.2

Table 4: Calibrated coefficients of the strength model, Equation (5)

Coefficient	Meaning	7-day	28-day
f_{c0} (N/mm²)	Control paste strength	33.20	41.71
m	Paste-decay exponent	80.0	80.0
B_f (N/mm²)	Bridging scale	994.7	1041.6
p_c	Optimum fibre fraction	0.069	0.073
R^2	Goodness of fit	0.811	0.887
RMSE (N/mm²)	Fit error	1.84	2.12

At 28 days, the model achieves $R^2 = 0.887$ with a root-mean-square error of 2.1 N/mm², and at 7 days $R^2 = 0.811$ with an error of 1.8 N/mm². Crucially, the bridging term places its optimum at $p_c \approx 7.3\%$ (28-day) and 6.9% (7-day), values obtained independently by the fitting routine, yet in close agreement with the experimentally observed strength peak at 6%. This independent recovery of the optimum dosage is strong evidence that Equation (5) reflects the real physics rather than merely tracing the data.

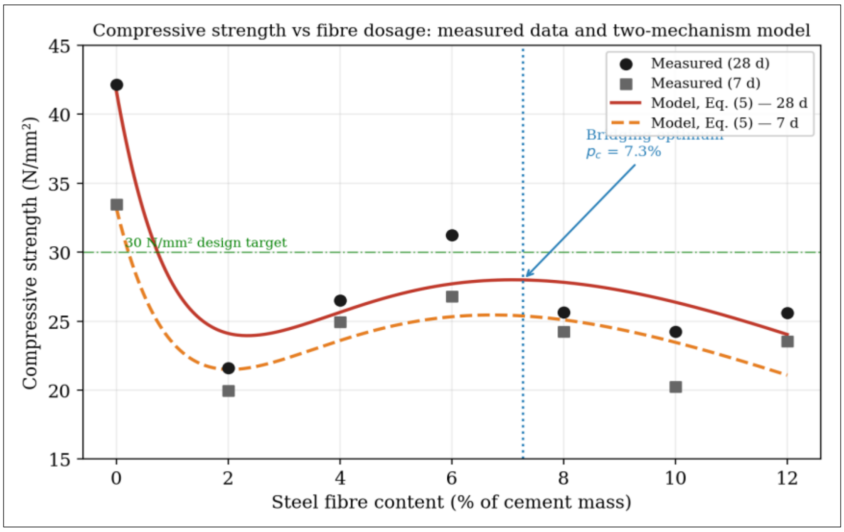

Figure 2: Compressive strength versus fibre dosage: Measured data and two-mechanism model

The residuals are small and show no systematic pattern, apart from the 2% mix, which lies below the fitted curve at both ages and carries the highest coefficient of variation among the fibre series; thus, its low value is consistent with test scatter.

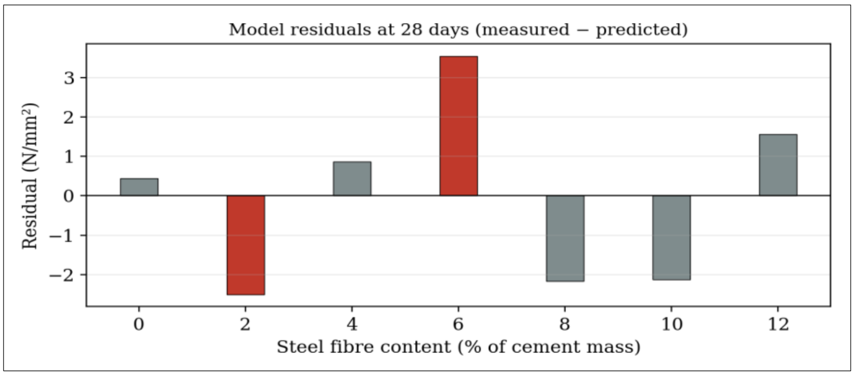

Figure 3: Model residuals at 28 days (measured minus predicted); the 2% mix is the only notable outlier.

5.4 Reliability assessment

Applying Equations (8) and (9) to the 28-day data shows that only the control mix clears the target with a comfortable margin ($\beta \approx 5.8$); every fibre mix falls below the 30 N/mm² characteristic requirement, with negative reliability indices. This is the direct structural consequence of the water-to-cement penalty in Equation (1) combined with the increased variability that fibre addition introduces. The 6% mix is the strongest of the fibre series and closest to the target, consistent with the optimum predicted by Equation (5).

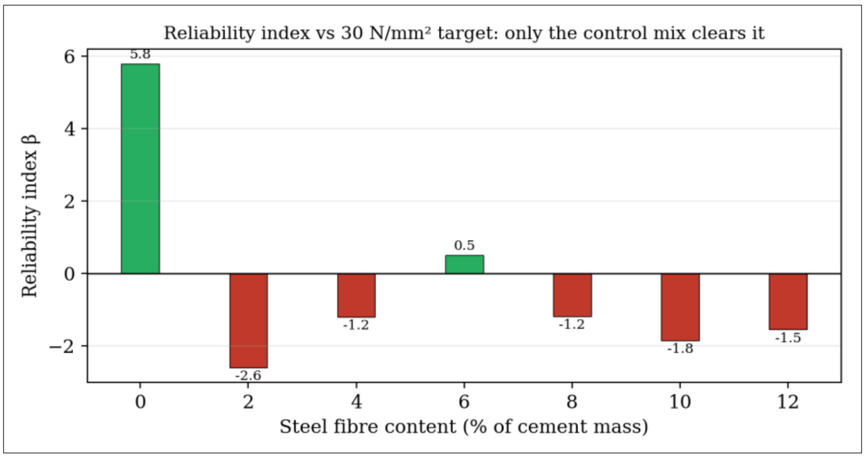

Figure 4: Reliability index for each mix relative to the 30 N/mm² target; only the control mix yields a positive index

5.5 Limitations and scope

The present programme comprises seven systematically spaced fibre dosages at two ages, sufficient to calibrate and interrogate the two-mechanism formulation but not to establish its coefficients as universal constants. The framework is therefore offered as a transferable methodology rather than a finalised design equation: the functional forms are mechanistically motivated and should generalise, but the fitted parameters will require recalibration for other matrices, fibre geometries and confinement conditions. Validation against independent datasets and against mixes in which fibres are added rather than replacing cement is the clear priority for subsequent work.

6. CONCLUSIONS

This study developed a transparent, mechanistically derived framework for steel fibre-reinforced concrete in which fibres replace cement by mass. The principal findings are:

1. The rising effective water-to-cement ratio, captured by Equation (1), is the dominant mechanism driving systematic strength loss as cement is replaced.
2. A two-mechanism model, Equation (5), predicts compressive strength as the sum of a paste-weakening term and a saturating crack-bridging term, reproducing the non-monotonic response at $R^2 = 0.887$ (28 days) and independently recovering the ~6–7% fibre optimum.
3. Hardened density showed no reliable dosage trend and is best described as bounded within the normal-weight band, Equation (10), rather than by an overfitted curve.
4. Propagation to characteristic strength and reliability indices shows that only the control mix clears the 30 N/mm² target; every fibre mix falls below it, owing to the combined water-to-cement penalty and increased variability.

The framework links predictive accuracy to structural usability and offers a reliability-based basis for specifying cement-replacing steel fibre content, with external validation identified as the priority next step.

Declarations

The author declares no conflict of interest. This manuscript is original, has not been published previously, and is not under consideration elsewhere.

Use of AI and AI-Assisted Technologies: An AI language model (Claude, Anthropic) was used to assist with restructuring and formatting of the manuscript. The underlying data, analysis, and scientific conclusions are entirely the author's own work, derived from the author's postgraduate research; the author reviewed and takes full responsibility for all AI-assisted edits.

REFERENCES

- Abbas, Y. M., & Khan, M. I. (2023). Robust machine learning framework for modelling the compressive strength of SFRC: Database compilation, predictive analysis, and empirical verification. *Materials, 16*(22), 7178. https://doi.org/10.3390/ma16227178
- Al-Shamasneh, A. R., Mahmoodzadeh, A., Karim, F. K., Saidani, T., Alghamdi, A., Alnahas, J., & Sulaiman, M. (2025). Application of machine learning techniques to predict the compressive strength of steel fiber reinforced concrete. *Scientific Reports, 15*, 30674. https://doi.org/10.1038/s41598-025-16516-1
- Alyousef, R., Rehman, M. F., Khan, M., Fawad, M., Khan, A. U., Hassan, A. M., & Ghamry, N. A. (2023). Machine learning-driven predictive models for compressive strength of steel fiber reinforced concrete subjected to high temperatures. *Case Studies in Construction Materials, 19*, e02418. https://doi.org/10.1016/j.cscm.2023.e02418
- Ben Chaabene, W., Flah, M., & Nehdi, M. L. (2020). Machine learning prediction of mechanical

properties of concrete: Critical review. *Construction and Building Materials, 260*, 119889. https://doi.org/10.1016/j.conbuildmat.2020.119889

- Garcia-Taengua, E., Bakhshi, M., & Ferrara, L. (2021). Meta-analysis of steel fiber-reinforced concrete mixtures leads to practical mix design methodology. *Materials, 14*(14), 3900. https://doi.org/10.3390/ma14143900
- Kang, M.-C., Yoo, D.-Y., & Gupta, R. (2021). Machine learning-based prediction for compressive and flexural strengths of steel fiber-reinforced concrete. *Construction and Building Materials, 266*, 121117. https://doi.org/10.1016/j.conbuildmat.2020.121117
- Köksal, F., Beycioğlu, A., & Dobiszewska, M. (2022). Optimization based on toughness and splitting tensile strength of steel-fiber-reinforced concrete incorporating silica fume using response surface method. *Materials, 15*(18), 6218. https://doi.org/10.3390/ma15186218
- Li, Y., Zhang, Q., Kamiński, P., Deifalla, A. F., Sufian, M., Dyczko, A., Ben Kahla, N., & Atig, M. (2022). Compressive strength of steel fiber-reinforced concrete employing supervised machine learning techniques. *Materials, 15*(12), 4209. https://doi.org/10.3390/ma15124209
- Mahesh, R., & Sathyan, D. (2022). Modelling the hardened properties of steel fiber reinforced concrete using ANN. *Materials Today: Proceedings, 49*, 2081–2089. https://doi.org/10.1016/j.matpr.2021.08.311
- Pakzad, S. S., Roshan, N., & Ghalehnovi, M. (2023). Comparison of various machine learning algorithms used for compressive strength prediction of steel fiber-reinforced concrete. *Scientific Reports, 13*, 3646. https://doi.org/10.1038/s41598-023-30606-y
- Premkumar, G., & Senthil Selvan, S. (2025). Prediction of mechanical properties of steel fibre-reinforced concrete under elevated temperature using artificial neural network techniques (ANN). *Frontiers in Built Environment, 11*, 1610115. https://doi.org/10.3389/fbuil.2025.1610115
- Stel'makh, S. A., Shcherban', E. M., Beskopylny, A. N., Mailyan, L. R., Meskhi, B., Razveeva, I., Kozhakin, A., & Beskopylny, N. (2022). Prediction of mechanical properties of highly functional lightweight fiber-reinforced concrete based on deep neural network and ensemble regression trees methods. *Materials, 15*(19), 6740. https://doi.org/10.3390/ma15196740
- Ullah, H. S., Khushnood, R. A., Ahmad, J., & Farooq, F. (2022). Predictive modelling of sustainable lightweight foamed concrete using machine learning novel approach. *Journal of Building Engineering, 56*, 104746. https://doi.org/10.1016/j.jobe.2022.104746
- Wang, Y., Jin, H., Demartino, C., Chen, W., & Yu, Y. (2022). Mechanical properties of SFRC: Database construction and model prediction. *Case Studies in Construction Materials, 17*, e01484. https://doi.org/10.1016/j.cscm.2022.e01484